X-ray second harmonic generation of systems with inversion symmetry

Ji-Cai Liu[1*], Catalin Miron[2,3], Hans Ågren[4,5], Sergei Polyutov[6], and Faris Gel'mukhanov[4,6]

[1] *Department of Mathematics and Physics, North China Electric Power University, 102206 Beijing, China*

[2] *Synchrotron SOLEIL, l'Orme des Merisiers, Saint-Aubin, BP 48, 91192 Gif-sur-Yvette Cedex, France*

[3] *Extreme Light Infrastructure Nuclear Physics (ELI-NP), 'Horia Hulubei' National Institute for Physics and Nuclear Engineering, 30 Reactorului Street, RO-077125 Măgurele, Judet Ilfov, Romania*

[4] *Theoretical Chemistry & Biology, School of Biotechnology, Royal Institute of Technology, S-106 91 Stockholm, Sweden*

[5] *Department of Physics and Astronomy, UppsalaUniversity, SE-75120Uppsala, Sweden*

[6] *Institute of Nanotechnology, Spectroscopy and Quantum Chemistry, Siberian Federal University, 660041 Krasnoyarsk, Russia*

[*] jicailiu@ncepu.edu.cn

Abstract

We explore the X-ray second harmonic generation process induced by resonant two-photon absorption in systems with inversion symmetry. We show that this process becomes allowed in the X-ray region due non-dipole contributions. We also show that while a plane wave pump field generates only a longitudinal second harmonic field, a gaussian pump beam creates also a transverse second harmonic field which is zero on the axis of pump beam and which is stronger than the longitudinal one and which, contrary to the longitudinal component, can run in free space. It is furthermore found that the second harmonic fields have radial polarization. Our theory is applied to Ar and Ne atomic vapours which have an energy conversion efficiency of X-ray SH generation 3.3×10^{-11} and 1.3×10^{-12}, respectively.

PACS numbers: 33.20.Rm, 33.80.Gj, 33.20.Fb, 32.80.Aa

Hans comments: 1) Faris, if X-ray SHG becomes allowed for symmetry inversion, then it woudl be applicable as a source for X-ray diffraction in crystals, like protein crystals ?

In this diamond experiment showing X-ray SHG, they must have concluded that one does not need inversion symmetry breaking ? How do they comment that (I cant dowload the paper from home) If so our paper gives an explanation rather than a prediction ?

Hans 2) HI Faris, the paper is not about SHG, it is fluorscence after two-photon absorption. SHG is a non-resonant process. We need to disicuss this tomorrow Hans

I. INTRODUCTION

Modern X-ray Free Electron Laser (XFEL) facilities can deliver high intensities $10^{15} - 10^{19} W/cm^2$ making it possible to significantly populate a core-excited state and even create population inversion and X-ray lasing[1–7]. At these intensities, X-ray matter interaction becomes nonlinear creating a room for studies of nonlinear effects like stimulated X-ray Raman scattering[3–5, 8–10], pulse compression [3–5] and X-ray four-wave mixing.[3–5, 11, 12] Glover et al[16] have demonstrated nonlinear wave mixing of X-ray and near-infrared beams. Second harmonic generation (SHG) is a nonlinear optical process of sum frequency generation which produces new photons with twice the frequency. SHG has traditionally been studied as an even-order nonlinear optical effect allowed in media without inversion symmetry[17] and is one of the best-understood nonlinear effects in optics[18]. In light of the XFEL development its study in the angstrom regime, e.g., on the natural scale of atomic and molecular structure of matter, has become of great interest both from a fundamental and practical viewpoint. A pioneering study by Shwartz, Yudovich et al[19, 20] gave recently experimental evidence for "off-resonant" SHG in diamond in the hard X-ray region with a pump frequency of 7.3 keV. In the present work we show that due to the large momentum of the photon $\mathbf{k}$ the nonlinearity in X-ray region is different from conventional nonlinearities in the visible regime and that SHG is generally possible possible to observe for centro-symmetric systems even when phase matching conditions do not prevail. We present a theoretical study of X-ray SHG in atomic gases induced by resonant two-photon absorption (TPA). We show that the plane wave pump field can create only longitudinally polarised X-ray second harmonic (SH) fields which can not propagate in free space (see however ref.[21]), but also that gaussian pump pulses induce in addiiton transverse second harmonic

fields which contrary to the longitudinal component can run in free space. Our idea is in a certain sense inverse to the use of longitudinal component of focussed light beams in laser particle accelerators[22]. Another important feature of studied SHG problem is that the transverse field, being strictly equal to zero on the beam axis, has an unusual radial polarization.

Our work is organized as follows. After this Introduction, we outline in the next SectionII A the basics theory of the SHG using plane-wave pump radiation which generates only the longitudinal field. Then, in the following SectionII B we show that the gaussian pump field creates also the transverse polarized SH field. SectionII C is devoted to the analysis of the longitudinally and radially polarised SH fields. We shed light on the role of the absorption of an SH field in SectionII D. Some theoretical details can be found in Appendices A and B. We disscuss our results further in Sec.III where we numerically analyse the efficiency of SHG in Ne and Ar vapours. Finally, in Sec.IV, we come to the conclusions.

II. THEORY

Quantum mechanically, the second order nonlinearity in the optical susceptibility originatse from a perturbational solution of the Schrödinger's equation. To get insight into the physics of the SHG process in X-ray region, we consider a propagation of an X-ray pump field $\mathbf{E}_p$ in an atomic gas far away from the absorption edge. To gain the SHG we choose twic ethe frequency of the pump field to be resonant with the frequency of a two-photon transition $2\omega \approx \omega_{10}$. The scheme of SHG is shown in Fig.1 where the pump field resonantly promotes the 1s electron of atom to the np unoccupied level. The resonant population of the state $|1\rangle$ in the course of TPA is followed by the emission of the SH field $\mathbf{E}$. Let us start from the atom-field interaction which in Coulomb gauge reads as (we use SI units)

$$V = V^{(1)} + V^{(2)} = -\frac{e}{mc}\mathbf{p}\cdot\boldsymbol{\mathcal{A}}_p + \frac{e^2}{2mc^2}\boldsymbol{\mathcal{A}}_p^2. \tag{1}$$

where m and e is the mass and charge of the electron, c is the speed of the light and $\mathbf{p}$ is the operator of electronic momentum. Below we will use more frequently the electric field instead of the vector potential, $\boldsymbol{\mathcal{E}} = -\partial\boldsymbol{\mathcal{A}}/\partial t$. The square of the vector potential of the pump field $\boldsymbol{\mathcal{A}}_p^2$ describes the TPA process in the first order of perturbation theory while the scalar product $\mathbf{p}\cdot\boldsymbol{\mathcal{A}}_p$ contributes in the TPA in second order of perturbation theory.

A. Plane wave pump field

It is instructive to consider first the interaction with the simplest and most fundamental electromagnetic wave, the transverse plane wave $\boldsymbol{\mathcal{A}}_p = (\mathbf{A}_p/2)\exp(-\imath(\omega t - \mathbf{k}\cdot\mathbf{r} - \mathbf{k}\cdot\mathbf{r}_e)) + c.c$

$$\begin{aligned} \boldsymbol{\mathcal{E}}_p &= \frac{1}{2}\mathbf{E}_p e^{-\imath(\omega t - \mathbf{k}\cdot\mathbf{r} - \mathbf{k}\cdot\mathbf{r}_e)} + c.c, \\ \mathbf{E}_p &= \mathbf{e}E_p^{(0)} = -\frac{\partial \mathbf{A}_p}{\partial t} = \imath\omega\mathbf{A}_p \end{aligned} \tag{2}$$

with the polarization $\mathbf{e}$ orthogonal to $\mathbf{k}$. Here $\mathbf{r}_e$ is the coordinate of the electron with respect to the atom and $\mathbf{r}$ ia the radius vector of atom in laboratory frame. To avoid an unnecessary complexity (see also below) we will focus only on the $\mathbf{A}_p^2$ term assuming that the wave length of the photon is longer than the size of core orbital $ka \ll 1$

$$V^{(2)} = \frac{e^2}{8mc^2}A^2 e^{-\imath 2(\omega t - \mathbf{k}\cdot\mathbf{r}_e - \mathbf{k}\cdot\mathbf{r})} \approx \frac{e^2}{8mc^2}A_p^{(0)2} e^{-\imath 2(\omega t - \mathbf{k}\cdot\mathbf{r})}(1 + \imath 2\mathbf{k}\cdot\mathbf{r}_e). \tag{3}$$

The term $A_p^{(0)2}$ being independent on the electron radius-vector $\mathbf{r}_e$ can not induce transitions between electronic states. Thus the transition between the ground (s) and core-excited (p) states is induced solely by the the matrix element

$$V_{01}^{(2)} \approx \imath\frac{eE_p^{(0)2}}{4mc^2\omega^2}(\mathbf{k}\cdot\mathbf{d}_{01})e^{-\imath 2(\omega t - \mathbf{k}\cdot\mathbf{r})} \tag{4}$$

of the second term $\mathbf{k}\cdot\mathbf{r}_e$ on the right-hand side of eq.(3). This pure non-dipole process opens the $s \to p$ TPA channel with the transition dipole moment $\mathbf{d}_{01} = e\mathbf{r}_{01} = e\langle 0|\mathbf{r}_e|1\rangle$ (Fig.1). We chose the axis z of quantization along the photon momentum $\mathbf{k}$. In this frame the pump field populates only the np_z level (see Fig.1) and the problem is reduced to the interaction with the two-level atom with the transition dipole moment parallel to the photon momentum

$$\mathbf{d}_{01} \parallel \mathbf{k}. \tag{5}$$

The resonant TPA population of the core-excited state of the p-symmetry is followed by the dipole allowed one-photon transition $p \to s$ which creates the SHG field with the double frequency 2ω. This explains why the SHG is possible in systems with inversion symmetry in the X-ray region.

To quantify the studied process one should compute the polarization $\boldsymbol{\mathcal{P}}$. The induced macroscopic polarisation of the medium being the expectation value of the dipole moment

$\mathbf{d}$ is specified in terms of the density matrix $\rho(t)$

$$\boldsymbol{\mathcal{P}} = N\mathrm{Tr}(\mathbf{d}\rho) = N\left(\mathbf{d}_{01}(t)\rho_{10}(t) + \mathbf{d}_{10}(t)\rho_{01}(t)\right), \tag{6}$$

where N is the concentration of atoms and $\mathbf{d}_{01}(t) = \mathbf{d}_{01}\exp(\imath\omega_{10}t)$ is the dipole moment in the interaction representation[22, 23]. The off-diagonal element of the density matrix $\rho_{10}(t) = \varrho_{10}\exp(-\imath(\nu t - 2\mathbf{k}\cdot\mathbf{r}))$ satisfies the following kinetic equation in the interaction picture[23]

$$\left(\frac{\partial}{\partial t} + \Gamma - \imath\nu\right)\varrho_{10} = \frac{1}{\hbar m}\Big(\frac{eE_p^{(0)}}{2\omega}\Big)^2(\mathbf{k}\cdot\mathbf{r}_{10})\left(\rho_{11} - \rho_{00}\right), \tag{7}$$

where $\nu = 2\omega - \omega_{10}$ is the detuning from the two-photon resonance and Γ is the lifetime broadening of core-excietd state $|1\rangle$. We neglect very weak depopulation of the ground state in the course of the two-photon absorption, ($\rho_{00} \approx 1$, $\rho_{11} \ll 1$) and assume that the duration τ of the pump pulse is longer than the lifetime of core excited state $1/\Gamma$. In this case one can use the stationary solution of eq.(7)

$$\varrho_{10} = \varrho_{10}^* = -\frac{1}{\hbar m}\left(\frac{eE_p^{(0)}}{2\omega}\right)^2\frac{(\mathbf{k}\cdot\mathbf{r}_{10})}{\Gamma - \imath\nu} \tag{8}$$

to find the induced macroscopic polarization taking into account eq.(5)

$$\begin{aligned}\boldsymbol{\mathcal{P}} &= \mathbf{P}\; e^{-\imath 2(\omega t - \mathbf{k}\cdot\mathbf{r})} + c.c., \\ \boldsymbol{P} &= \hat{\mathbf{k}}p, \quad p = -\left(\frac{eE_p^{(0)}}{2\omega}\right)^2\frac{Nker_{01}^2}{m\hbar(\Gamma - \imath\nu)}.\end{aligned} \tag{9}$$

Here $\hat{\mathbf{k}} = \mathbf{k}/k$ is the unit vector along $\mathbf{k}$. One can see that the pump radiation creates a macroscopic polarisation $\boldsymbol{\mathcal{P}}$ oriented along the direction of propagation of the pump field $\mathbf{k}$ and, hence of the SH field $\boldsymbol{\mathcal{E}}$, which is created in the course of the spontaneous transition $|1\rangle \to |0\rangle$ whic also is parallel to $\mathbf{k}$. This longitudinal field exists everywhere where there is pump-field and the medium and this field copies exactly the polarization according to Maxwell's equation for the induction, $\mathrm{div}\boldsymbol{\mathcal{D}} = \partial(\epsilon_0\mathcal{E} + \mathcal{P})/\partial z = 0$:

$$\mathbf{E} = -\frac{2}{\epsilon_0}\mathbf{P} \neq 0, \quad \boldsymbol{\mathcal{D}} = 0, \quad \boldsymbol{\mathcal{H}} = 0. \tag{10}$$

This does not contradict the well known fact that the plane wave longitudinal field does not exist in free space[21]. This statement means that longitudinal field can not propagate in free space. Indeed, the here studied case is different. The longitudinal field $\boldsymbol{\mathcal{E}}$ exists only in

the region where the pump field creates longitudinal polarization $\boldsymbol{\mathcal{P}} \propto \mathbf{k}$. This longitudinal field oscillating in time and space is a pure electric field, $\boldsymbol{\mathcal{H}} = 0$.

As we have already noticed above the TPA process is a first-order process with respect to $\boldsymbol{\mathcal{A}}_p^2$ and a second-order process with respect to $\mathbf{p} \cdot \boldsymbol{\mathcal{A}}_p$. Here we study the two-photon transition $s \to p$ which is a pure non-dipole effect. Since both $\boldsymbol{\mathcal{A}}_p^2$ and $\mathbf{p} \cdot \boldsymbol{\mathcal{A}}_p$ induced TPA result in the same orientation of the TPA induced polarization we consider here only the $\boldsymbol{\mathcal{A}}_p^2$ contribution. The taking into account of the $\mathbf{p} \cdot \boldsymbol{\mathcal{A}}_p$ TPA process will result only in a rescaling (increase) of the SHG efficiency.

B. Gaussian pump beam and paraxial equation

In this section we will show that the pump Gaussian pump beam makes it possible

$$\begin{aligned} \boldsymbol{\mathcal{E}}_p &= \frac{1}{2}\mathbf{E}_p e^{-\imath(\omega t - kz)} + c.c., \\ \mathbf{E}_p &= \hat{\mathbf{x}} E_p^{(0)} g\left(t - \frac{z}{c}\right) \frac{w_0}{w_(z)} \exp\left(-\frac{\varrho^2}{w^2(z)}\right) \exp\left(\imath\left(k\frac{\varrho^2}{2R(z)} - \psi(z)\right)\right) \end{aligned} \tag{11}$$

to transform the longitudinal SHG X-ray field into a transfer field which can propagate in free space in contrast to the pure longitudinal field. Eq.(11) identifies $R(z) = z\left(1 + (z_R/z)^2\right)$ as the radius of curvature of the wavefront of the beam at z, w_0 as the beam waist and $g(t) = \exp(-t^2/2\tau^2)$ as the temporal shape of the pulse with duration τ. Here $w(z) = w_0\sqrt{1 + (z/z_R)^2}$, $\psi(z) = \arctan(z/z_R)$, $\rho = \sqrt{x^2 + y^2}$, $w_0/z_R \ll 1$. The gaussian beam remains well collimated up to the the Rayleigh range $z_R = kw_0^2/2$ (Fig.2).

Since the wavefront is not orthogonal to z as one can see from the phase $\phi = 2k(z + \rho^2/2R)$ of $E_p^2 \propto \exp(\imath\phi)$, that the polarization $\mathbf{P}$ is slightly tilted from the z-axis. To find the matrix element $V_{01}^{(2)}$ of the interaction with the pump gaussian beam (11) we need the value of this interaction at the point of the electron $\mathbf{r}_e$ with respect to the atom $\mathbf{r} = (\boldsymbol{\rho}, z) \to \mathbf{r} + \mathbf{r}_e$.

$$\langle 0|e^{\imath(\phi+\delta\phi)}|1\rangle \approx e^{\imath\phi}\langle 0|1 + \imath\delta\phi|1\rangle = \boldsymbol{\kappa} \cdot \langle 0|\mathbf{r}_e|1\rangle e^{\imath\phi}\, \imath 2k, \tag{12}$$

where $\delta\phi = \boldsymbol{\nabla}\phi \cdot \mathbf{r}_e$. Similar to the derivation of eq.(9) one obtains a polarisation that is oriented along $\boldsymbol{\nabla}\phi \equiv (\partial_z\phi, \partial_\rho\phi) = 2k\boldsymbol{\kappa}$

$$\mathbf{P} = -\boldsymbol{\kappa}\left(\frac{eE_p}{2\omega}\right)^2 \frac{Nker_{01}^2}{m\hbar(\Gamma - \imath\nu)}, \quad \boldsymbol{\kappa} = \hat{\mathbf{z}} + \hat{\boldsymbol{\rho}}\frac{\rho}{R} \tag{13}$$

instead of the beam axis $\hat{\mathbf{z}} \parallel \mathbf{k}$.

Let us write the optical wave equation for the SHG field $\boldsymbol{\mathcal{E}}$

$$\boldsymbol{\nabla}(\boldsymbol{\nabla}\cdot\boldsymbol{\mathcal{E}})-\boldsymbol{\nabla}^2\boldsymbol{\mathcal{E}}+\frac{1}{c^2}\frac{\partial^2\boldsymbol{\mathcal{E}}}{\partial t^2}=-\mu_0\frac{\partial^2\boldsymbol{\mathcal{P}}}{\partial t^2} \tag{14}$$

in the usual manner[18] starting from the couple of Maxwell's equations (in SI units) for nonmagnetic materials (μ=1)

$$\boldsymbol{\nabla}\times\boldsymbol{\mathcal{E}}=-\mu_0\frac{\partial\boldsymbol{\mathcal{H}}}{\partial t},\quad \boldsymbol{\nabla}\times\boldsymbol{\mathcal{H}}=\frac{\partial\boldsymbol{\mathcal{D}}}{\partial t}. \tag{15}$$

Contrary to conventional theories[18] for the transfer electromagnetic field where $\boldsymbol{\nabla}\cdot\boldsymbol{\mathcal{E}}=$ div$\boldsymbol{\mathcal{E}}=0$ we can not ignore $\boldsymbol{\nabla}\cdot\boldsymbol{\mathcal{E}}$. This is because the polarization $\boldsymbol{\mathcal{P}}$ is essentially a longitudinal one (see eq.(13)): div$\boldsymbol{\mathcal{P}}\neq 0$. To resolve this problem we use the Maxwell's equation for the induction $\boldsymbol{\mathcal{D}}=\varepsilon_0\boldsymbol{\mathcal{E}}+\boldsymbol{\mathcal{P}}$

$$\boldsymbol{\nabla}\cdot\boldsymbol{\mathcal{D}}=0,\quad \boldsymbol{\nabla}\cdot\boldsymbol{\mathcal{E}}=-\frac{1}{\epsilon_0}\boldsymbol{\nabla}\cdot\boldsymbol{\mathcal{P}}, \tag{16}$$

which makes it possible to rewrite the wave equation (14) as follows

$$\begin{aligned}&-\boldsymbol{\nabla}^2\boldsymbol{\mathcal{E}}+\frac{1}{c^2}\frac{\partial^2\boldsymbol{\mathcal{E}}}{\partial t^2}=\frac{1}{\epsilon_0}\left(-\frac{1}{c^2}\frac{\partial^2\boldsymbol{\mathcal{P}}}{\partial t^2}+\boldsymbol{\nabla}(\boldsymbol{\nabla}\cdot\boldsymbol{\mathcal{P}})\right),\\ &\boldsymbol{\mathcal{E}}=\frac{1}{2}\mathbf{E}e^{-\imath 2(\omega t-kz)}+c.c.,\quad \boldsymbol{\mathcal{P}}=\mathbf{P}e^{-\imath 2(\omega t-kz)}+c.c..\end{aligned} \tag{17}$$

This wave equation differs from the conventional one [18] by the extra term $\boldsymbol{\nabla}(\boldsymbol{\nabla}\cdot\boldsymbol{\mathcal{P}})\neq 0$ which is not equal to zero because of the longitudinal contribution in $\boldsymbol{\mathcal{P}}$. We would like to point out that when the pump field is a plane wave there is only a longitudinal SH field $\boldsymbol{\mathcal{E}}\parallel z$ (see Sec.II A). In this case the wave equation (14) becomes $\partial^2(\epsilon_0\boldsymbol{\mathcal{E}}+\boldsymbol{\mathcal{P}})/\partial t^2=0$, which is very different from eq.(17) because $\boldsymbol{\nabla}(\boldsymbol{\nabla}\cdot\boldsymbol{\mathcal{E}})-\boldsymbol{\nabla}^2\boldsymbol{\mathcal{E}}=(\partial^2/\partial z^2-\partial^2/\partial z^2)\mathcal{E}\equiv 0$.

Now we are in a stage to simplify the wave equation (17). In our case the wave is propagating primarily along the z-axis with a small divergence angle

$$\theta\approx\frac{1}{kw_0}=\frac{2w_0}{z_R}\sim\frac{\lambda}{\omega_0}\ll 1. \tag{18}$$

This makes it possible to neglect $\partial^2\mathcal{A}/\partial z^2$ in eq. (17) and to get the following paraxial equation for the SHG field

$$\left(\frac{\partial}{\partial z}+\frac{1}{c}\frac{\partial}{\partial t}-\frac{\imath}{4k}\Delta_\perp\right)\mathbf{E}=\frac{\imath}{2k}\mathbf{f}e^{\imath 2(\omega t-kz)}, \tag{19}$$

where $\Delta_\perp = \boldsymbol{\nabla}_\rho^2 = \partial^2/\partial x^2 + \partial^2/\partial y^2$ is the Laplacian operator over transverse cartesian coordinates. The source term on the right-hand side of the paraxial equation has now both longitudinal (f_z) and transverse components (f_ρ)

$$\begin{aligned}
&\mathbf{f} = \hat{\mathbf{z}} f_z + \hat{\boldsymbol{\rho}} f_\rho, \\
&\mathbf{f} = \frac{2}{\epsilon_0}\left(-\frac{1}{c^2}\frac{\partial^2 \tilde{\mathbf{P}}}{\partial t^2} + \boldsymbol{\nabla}(\boldsymbol{\nabla}\cdot\tilde{\mathbf{P}})\right) \approx \frac{2}{\epsilon_0}\left((2k)^2\tilde{\mathbf{P}} + \boldsymbol{\nabla}(\boldsymbol{\nabla}\cdot\tilde{\mathbf{P}})\right), \\
&\tilde{\mathbf{P}} = \mathbf{P} e^{-\imath 2(\omega t - kz)}.
\end{aligned} \tag{20}$$

Taking into account eqs.(11), (13) and (18) one can get the following expression for the transverse and longitudinal components of $\mathbf{f}$

$$\begin{aligned}
f_\rho &= -\frac{\imath 16 k\rho}{\epsilon_0 w^2} P, \\
f_z &= \frac{\imath 4kP}{\epsilon_0(z^2+z_R^2)}\Big[\frac{2k\rho^2 z_R(\imath z_R + z)}{z^2+z_R^2} - \imath 4 z_R - z\Big].
\end{aligned} \tag{21}$$

One should point out that origin of the f_ρ is the term $\boldsymbol{\nabla}(\boldsymbol{\nabla}\cdot\tilde{\mathbf{P}}) = \hat{\boldsymbol{\rho}}\partial_\rho(\partial_z\tilde{P}) + \cdots$. A simple estimation shows that the transverse contribution dominates: $|f_\rho/f_z| \sim kw_0 \gg 1$. As one can see from the paraxial equation (19) the transverse and longitudinal components of $\mathbf{f}$ generate, respectively, the transverse and longitudinal components of the SH field $\mathbf{E}$.

C. Spatial distribution of the transverse and longitudinal SH fields. Radial polarization

The solution of the paraxial equation (19) is convenient to write in terms of the retarded Green's function (see Appendix A)

$$\begin{aligned}
&\mathbf{E}(z,\boldsymbol{\rho},t) = \frac{1}{2\pi}\int G(z-z',\boldsymbol{\rho}-\boldsymbol{\rho}',t-t')\tilde{\mathbf{f}}(z',\boldsymbol{\rho}',t')dz'd\boldsymbol{\rho}'dt', \\
&\left(\frac{\partial}{\partial z} + \frac{1}{c}\frac{\partial}{\partial t} - \frac{\imath}{4k}\Delta_\perp\right) G(z-z',\boldsymbol{\rho}-\boldsymbol{\rho}',t-t') = \delta(z-z')\delta(\boldsymbol{\rho}-\boldsymbol{\rho}')\delta(t-t')\Theta(t-t'). \\
&G(z-z',\boldsymbol{\rho}-\boldsymbol{\rho}',t-t') = -\imath\delta\left(t'-t-\frac{z'-z}{c})\right)\Theta(t-t')\frac{k}{\pi(z-z')}\exp\left(\imath\frac{k|\boldsymbol{\rho}-\boldsymbol{\rho}')^2}{z-z'}\right),
\end{aligned} \tag{22}$$

which guarantees that no contribution at remotely early times , t, before the source $\tilde{\mathbf{f}}(z',\boldsymbol{\rho}',t') = \mathbf{f}(z',\boldsymbol{\rho}',t')\exp(\imath 2(\omega t' - kz'))$ has been activated. Taking into account that $\hat{\mathbf{z}}' = \hat{\mathbf{z}}$, $\hat{\boldsymbol{\rho}}' = \hat{\boldsymbol{\rho}}\cos\varphi + \hat{\mathbf{y}}\sin\varphi$, $\hat{\mathbf{y}} \perp \hat{\boldsymbol{\rho}}$, one can perform an integration over directions of $\boldsymbol{\rho}'$

using eq.(A5)

$$\int_0^{2\pi} d\varphi[\hat{\boldsymbol{\rho}}' f_\rho(z',\rho',t') + \hat{\mathbf{z}} f_z(z',\rho',t')] \exp\left(\imath \frac{k|\boldsymbol{\rho}-\boldsymbol{\rho}')^2}{z-z'}\right) \tag{23}$$
$$= 2\pi \exp\left(\imath \frac{k(\rho^2+\rho'^2)}{z-z'}\right)\Big[- \hat{\boldsymbol{\rho}}\imath f_\rho(z',\rho',t') J_1\left(\frac{2k\rho\rho'}{z-z'}\right) + \hat{\mathbf{z}} f_z(z',\rho',t') J_0\left(\frac{2k\rho\rho'}{z-z'}\right)\Big],$$

where $J_n(x)$ is a Bessel function. One can obtain the remaining integral over ρ' using eq.(A5) and get the following expressions for transfers and longitudinal contributions

$$\mathbf{E}(z,\boldsymbol{\rho},t) = \hat{\boldsymbol{\rho}} E_\rho(z,\boldsymbol{\rho},t) + \hat{\mathbf{z}} E_z(z,\boldsymbol{\rho},t), \tag{24}$$
$$E_i(z,\rho,t) = E_p^{(0)} g^2\left(t - \frac{z}{c}\right) J_i(z,\rho), \quad i = (\rho, z),$$

where

$$J_\rho(z,\rho) = -2\rho s_0 \int_{-\infty}^{z} dz' \frac{e^\Phi}{w^4(z')\alpha^2(z')}, \tag{25}$$
$$J_z(z,\rho) = \frac{\imath 4\pi w_0 s_0}{(kw_0)^3} \int_{-\infty}^{z} dz' \frac{e^\Phi}{w^4(z')\alpha(z')}\left[\frac{2(\imath z_R + z')}{w^2(z')\alpha(z')}\left(z - z' - \frac{2k^2\rho^2}{\alpha(z')}\right) - (\imath 4 z_R + z')\right],$$
$$\Phi = \frac{\imath k\rho^2}{z-z'} - \imath 2\psi(z') - \frac{k^2\rho^2}{(z-z')\alpha(z')}, \quad \alpha(z') = \frac{2(z-z')}{w^2(z')} - \imath k\left(\frac{z-z'}{R(z')} + 1\right),$$
$$s_0 = 8\pi \frac{G}{\Gamma - \imath\nu} N z_R r_{01} r_e$$

Here $r_e = e^2/(4\pi\epsilon_0 mc^2) = 2.82 \times 10^{-13}$ cm is the classical electron radius and $G = E_p^{(0)} d_{01}/\hbar$ is the Rabi frequency. It is important to notice that there is no transverse field on the beam axis

$$E_\rho(z, \rho = 0, t) = 0. \tag{26}$$

Eq.(24) indicates that the transverse SH field $\hat{\boldsymbol{\rho}} E_\rho$ is oriented along the radius $\boldsymbol{\rho}$ perpendicular to the beam axis. This means that the transverse field has radial polarization (see also Sec.III).

D. Role of photoabsorption

In the above equations the photoabsorpion of X-rays is ignored. This approximation is valid for the pump beam which is far from any resonance. In contrast, the SHG field is in

strict resonance with the dipole allowed transition $|0\rangle \to |1\rangle$ (1s-3p for Ne and 1s-4p for Ar). Therefore, this absorption channel should be taken into account. With the solution (24) at hand we are almost prepared to include the photoabsorption in the SH field. As it is shown in Appendix B the photoabsorption of the SHG field modifies only the integrands at the right-hand side of equations (25) for $J_\rho(z,\rho)$ and $J_z(z,\rho)$. Namely, these integrands should be multiplied by the factor

$$\exp\left(\frac{z'-z}{2\ell}\right), \tag{27}$$

where $\ell = 1/N\sigma_{\rm abs}$ is the photoabsorption length while $\sigma_{\rm abs}$ is the the resonant photoabsorption cross section. According to simulations the photoabsorption length should be larger or comparable with the Rayleigh range

$$\ell \sim z_R \tag{28}$$

to make it possible for the SHG field reach the optimal value.

III. RESULTS OF SIMULATIONS AND DISCUSSION

We applied the theory to two atomic system, Ne and Ar, with the strict two-photon resonance ($2\omega = \omega_{10}$) with $1s \to 3p$ transitions for Ne and $1s \to 4p$ transitions for Ar. In the simulations with the peak pump intensity $I_p^{(0)} = c\epsilon_0|E_p^{(0)}|^2/2 = 10^{16}W/cm^2$ we used the following parameters for Ne: $\hbar\omega_{1s-3p} = 867.4$ eV, $\sigma_{\rm abs}(1s-3p) = 1.5\times10^{-18}cm^2$[24], $2\hbar\Gamma = 0.27$ eV [25] and for Ar: $\hbar\omega_{1s-4p} = 3203.42$ eV, $\sigma_{\rm abs}(1s-4p) = 0.12\times10^{-18}cm^2$[26], $2\hbar\Gamma = 0.66$ eV[27]. The concentration of the atoms and the beam waist were equal to $N = 10^{19}cm^{-3}$ and $w_0 = 1\mu m$, respectively. The Rayleigh range was $z_R \approx 10^3\mu m$ and $z_R \approx 4\times10^3\mu m$ for Ne and Ar, respectively. The corresponding values of the photoabsorption lengths $\ell \approx 0.67\times10^3\mu m$ and $8\times10^3\mu m$ satisfy the condition (28).

We deliberately solved the paraxial equation with homogeneous distribution of the concentration along the z-axis. This makes it possible to easily to estimate the size of the gas cell. We characterize the SHG by its intensity distribution of the transverse and longitudinal components of the SH field (24).

$$I_i(z,\rho,t) = \frac{1}{2}c\epsilon_0|E_i(z,\rho,t)|^2, \quad i = (\rho, z) \tag{29}$$

and by the energy conversion efficiency

$$\beta_i = \frac{W_i(z)}{W_p}, \quad W_i(z) = 2\pi\int_0^\infty dt\int_0^{2\pi} d\rho I_i(z,\rho,t). \tag{30}$$

First we show the SH field neglecting the photoabsorption. In Fig.3 and Fig.4 we display the spatial distribution of the SH intensities $I_\rho(z,\rho,t)$ and $I_z(z,\rho,t)$ for Ne and Ar, respectively. One can see that the transverse SH field I_ρ is much stronger than longitudinal one I_z and $I_\rho = 0$ on the axis of the beam $\rho = 0$. The transverse field $\hat{\boldsymbol{\rho}} E_\rho$ (24) has an unusual radial polarization as is shown in Fig.6. The photobasorption changes dramatically the spatial distribution of the SH field. The photoabsorption also reduces the energy conversion efficiency, in one order of magnitude for Ne and in four times for Ar, as one can see from Fig. 5 and Fig.8. As it is expected the SH field is confined in the focal region in the range limited by the photobasorption length ℓ (see Fig. 7). Due to this circumstance the energy conversion efficiency becomes maximal at $z = z_{\max} = 0.7$ mm for Ne and $z_{\max} = 0.5$ cm for Ar. This range defines the size of the gas cell which should be around $z_{\max}$.

IV. SUMMARY

In this paper, we investigated the second harmonic generation in systems with the inversion symmetry in the X-ray region. Our theory is applied to SHG in neon and argon pumped by a strong X-ray field tuned in resonance with the two-photon transition $1s \to 3p$ in Ne and $1s \to 4p$ in Ar. The non-dipole population of these core-excited states is followed by the emission of the SH field. We describe the SHG in atoms in terms of a density matrix formalism and paraxial equation taking into account the resonant photobasorption of the SH radiation. I contrast to the plane wave pump field, the gaussian pump beam generates transverse SH photons with the radial polarization. Theory predicts the energy conversion efficiency 10^{-11} and 10^{-12} in Ne (867.4 eV) and Ar (3203.4 eV) atomic vapours for the pump 10^{16} W/cm^3, respectively.

Acknowledgements. The research leading to these results has received funding from a public grant from the Laboratoire d'Excellence Physics Atoms Light Matter (LabEx PALM) and from the Laboratoire d'Excellence MiChEm. and from the Swedish Research Council (VR). J.-C. Liu thanks the support by the National Science Foundation of China under grant Nos. 11574082 and 11204078, and the Fundamental Research Funds for the Central Universities under grant No. 2018MS050. FG and SP acknowledge support within the State contract of the Russian Federation Ministry of Education and Science for Siberian Federal University for scientific research in 2017-2019 (Project 3.2662.2017). HÅ acknowledges The

Knut and Alice Wallenberg foundation for financial support (Grant No. KAW-2013.0020).

Appendix A: Green's function for the time-dependent paraxial equation

Let us find the Green's function of non-stationary paraxial equation

$$\left(\frac{\partial}{\partial z}+\frac{1}{c}\frac{\partial}{\partial t}-\frac{\imath}{2K}\Delta_\perp\right)G(z,\boldsymbol{\rho},t)=\Theta(t)\delta(t)\delta(z)\delta(\boldsymbol{\rho}), \tag{A1}$$

where $\Delta_\perp=\partial^2/\partial x^2+\partial^2/\partial y^2$, $\boldsymbol{\rho}=(x,y)$, $\delta(\boldsymbol{\rho})=\delta(x)\delta(y)$ and $\Theta(t)$ is the step function which is equal to zero when $t<0$. Taking the Fourier transform of the Green's function and of the Dirac δ-functions we get

$$\begin{aligned}
&G(z,\boldsymbol{\rho},t)=\frac{\Theta(t)}{(2\pi)^4}\int\limits_{-\infty}^{\infty}d\mu\int\limits_{-\infty}^{\infty}d\nu\int\limits_{-\infty}^{\infty}dp\int\limits_{-\infty}^{\infty}dqG_{\mu,\nu,p,q}e^{\imath\mu t+\imath\nu z+\imath px+\imath qy},\\
&G_{\mu,\nu,p,q}=-\frac{2\imath}{\frac{\mu}{c}+\nu+\frac{p^2+q^2}{2K}}.
\end{aligned} \tag{A2}$$

Keeping in mind that $t\geq 0$ and taking the integral along half circle in upper half plane around the pole $\mu=-c\left(\nu+\frac{p^2+q^2}{2K}\right)$

$$\int\limits_{-\infty}^{\infty}\frac{e^{\imath\mu t}}{\frac{\mu}{c}+\nu+\frac{p^2+q^2}{2K}}d\mu=-\imath c\pi\exp\left(-\imath ct\left(\nu+\frac{p^2+q^2}{2K}\right)\right), \tag{A3}$$

we obtain the following expression for the Green's function

$$G(z,\boldsymbol{\rho},t)=-\imath\delta\left(t-\frac{z}{c}\right)\Theta(t)\frac{K}{2\pi z}\exp\left(\imath\frac{K\rho^2}{2z}\right) \tag{A4}$$

which allows to find the SHG field (22) with help of the following integrals[28]

$$\begin{aligned}
&J_0(a)=\frac{1}{2\pi}\int_0^{2\pi}e^{\imath a\cos\theta}d\theta,\\
&\frac{1}{2\pi}\int_0^{2\pi}\cos\theta e^{-\imath a\cos\theta}d\theta=\imath\frac{d}{da}J_0(a)=-\imath J_1(a),\\
&\int\limits_0^{\infty}e^{-a^2\rho^2}\rho^{n+1}J_n(b\rho)d\rho=\frac{b^n}{(2a^2)^{n+1}}e^{-\frac{b^2}{4a^2}},\quad \mathrm{Re}(a^2)>0.
\end{aligned} \tag{A5}$$

Appendix B: Photoabsorption of SHG field

The strongest absorption channel is the absorption of SH field which is in the resonance with $|0\rangle\rightarrow|1\rangle$ transition. To account this photoabsorption we need to add $-\mathbf{E}/2\ell$ at the

right-hand side of paraxial equation (19)

$$\left(\frac{\partial}{\partial z}+\frac{1}{c}\frac{\partial}{\partial t}-\frac{\imath}{4k}\Delta_{\perp}\right)\mathbf{E}=-\frac{1}{2\ell}\mathbf{E}+\frac{\imath}{2k}\mathbf{f}e^{\imath 2(\omega t-kz)}, \tag{B1}$$

where $\ell=1/\sigma N$ is the length of resonant absorption of the SHG field with the photoabsorption cross-section σ. Using the substitution $\mathbf{E}=\tilde{\mathbf{E}}\exp(-z/2\ell)$ one can see that $\tilde{\mathbf{E}}$ satisfies paraxial equation (19)

$$\left(\frac{\partial}{\partial z}+\frac{1}{c}\frac{\partial}{\partial t}-\frac{\imath}{4k}\Delta_{\perp}\right)\tilde{\mathbf{E}}=\frac{\imath}{2k}\mathbf{f}e^{\imath 2(\omega t-kz)}e^{z/2\ell} \tag{B2}$$

with modified source term. This equation has the solution given by eq.(22) with $\tilde{\mathbf{f}}$ replaced by $\tilde{\mathbf{f}}\exp(z'/2\ell)$. Taking into account this we get immediately the solution of paraxial equation with photoabsorption (B1)

$$\mathbf{E}(z,\boldsymbol{\rho},t)=\tilde{\mathbf{E}}e^{-z/2\ell}=\frac{e^{-z/2\ell}}{2\pi}\int G(z-z',\boldsymbol{\rho}-\boldsymbol{\rho}',t-t')\tilde{\mathbf{f}}(z',\boldsymbol{\rho}',t')e^{z'/2\ell}dz'd\boldsymbol{\rho}'dt'. \tag{B3}$$

This means that to account the photoabsorption we should multiply by $\exp((z'-z)/2\ell)$ the integrand at the right-hand side of equations (25) for $J_{\rho}(z,\rho)$ and $J_z(z,\rho)$.

---

[1] N. Rohringer and R. London, *Phys. Rev. A*, **80**, 013809 (2009).

[2] N. Rohringer, D. Ryan, R. London, M. Purvis, F. Albert, J. Dunn, J.D. Bozek, C. Bostedt, A. Graf, R. Hill, S.P. Hau-Riege, and J.J. Rocca, *Nature* **481**, 488 (2012).

[3] Y.-P. Sun, J.-C. Liu, and F. Gel'mukhanov, *Euro Phys. Lett.*, **87**, 64002 (2009).

[4] Y.-P. Sun, J.-C. Liu, and F. Gel'mukhanov, *J. Phys.B: At.Mol.Opt.Phys.*, **42**, 201001 (2009).

[5] Y.-P. Sun, J.-C. Liu, C.-K. Wang, and F. Gel'mukhanov, *Phys. Rev. A*, **81**, 013812 (2010).

[6] Q. Miao, J.-C. Liu, H. Ågren, J-E. Rubensson, and F. Gel'mukhanov, Dissociative X-ray Lasing, *Phys. Rev. Lett.*, **109**, 233905 (2012).

[7] V. Kimberg and N. Rohringer, Amplified X-ray Emission from Core-Ionized Diatomic Molecules, *Phys. Rev. Lett.*, **110**, 043901 (2013).

[8] V. Kimberg and N. Rohringer, Stochastic stimulated electronic X-ray Raman spectroscopy, *Structural Dynamics*, **3**, 034101 (2016).

[9] V. Kimberg, A. Sanchez-Gonzalez, L. Mercadier, C. Weninger, A. Lutman, D. Ratner, R. Coffee, M. Bucher, M. Mucke, M. Agåker, C. Såthe, C. Bostedt, J. Nordgren, J.-E. Rubensson,

and N. Rohringer, Stimulated X-ray Raman scattering: a critical assessment of the building block of nonlinear X-ray spectroscopy, *Faraday discussions*, **194**, 305-324, (2016).

[10] M. Beye, S. Schreck, F. Sorgenfrei, C. Trabant, N. Pontius, S. Schüßler-Langeheine, W. Wurth, and A. Föhlisch, Stimulated X-ray emission for materials science, Nature, **501**, 191-194 (2013)

[11] S. Tanaka and S. Mukamel, *Phys. Rev. Lett.*, **89**, 043001 (2002).

[12] S. Mukamel, *Phys. Rev. B*, **72**, 235110 (2005).

[13] N. Rohringer and R. Santra, *Phys. Rev. A*, **77**, 053404 (2008).

[14] J.-C. Liu, Y.-P. Sun, C.-K. Wang, H. Ågren, and F. Gel'mukhanov, *Phys. Rev. A*, **81**, 043412 (2010).

[15] Y.-P. Sun, Q. Miao, A.-P. Zhou, R.-J. Liu, B. Liu, and F. Gel'mukhanov, Suppression of resonant auger effect with chirped x-ray free-electron laser pulse, *J. Phys. B: At.Mol.Opt.Phys.* **51**, 035602 (2018).

[16] T. E. Glover, D.M. Fritz, M. Cammarata, T.K. Allison, S. Coh, J.M. Feldkamp, H. Lemke, D. Zhu, Y. Feng, R.N. Coffee, M. Fuchs, S. Ghimire, J. Chen, S. Shwartz, D.A. Reis, S.E. Harris, and J.B. Hastings, X-ray and optical wave mixing, *Nature*, **488**, 603 (2012).

[17] P. Franken, A. Hill, C. Peters, and G. Weinreich, "Generation of Optical Harmonics". *Phys. Rev. Lett.* **7**, 118 (1961)

[18] R.W. Boyd, *Nonlinear Optics*, Academic Press, Elsevier, Singapore, 2010.

[19] S. Shwartz, M. Fuchs, J. B. Hastings, Y. Inubushi, T. Ishikawa, T. Katayama, D. A. Reis, T. Sato, K. Tono, M. Yabashi, S. Yudovich, and S. E. Harris, X-Ray Second Harmonic Generation, *Phys. Rev. Lett.*, **112**, 163901 (2014).

[20] S. Yudovich and S. Shwartz. Second-harmonic generation of focused ultrashort x-ray pulses. *Journal of the Optical Society of America B*, **32**, 1894-1900 (2015).

[21] T. F. Heinz and D. P. DiVincenzo, Comment on "Forbidden nature of multipolar contributions to second-harmonic generation in isotropic fluids", *Phys. Rev. A*, **42**, 6249-6251 (1990).

[22] M. O. Scully and M. S. Zubairy, Simple laser accelerator: Optics and particle dynamics, *Phys. Rev. A*, **44**, 2656-2663 (1991).

[23] P.W. Milonni and J.H. Eberly, *Lasers Physics*, John Wiley & Sons, New York, 2010.

[24] C. Buth, R. Santra, and L. Young, Electromagnetically Induced Transparency for X-rays, *Phys. Rev. Lett.*, **98**, 253001 (2007).

[25] V. Schmidt, *Electron Spectrometry of Atoms Using Synchrotron Radiation*, Cambridge Uni-

versity Press, Cambridge, England, 1997.

[26] C. Buth and R. Santra, X-ray refractive index of laser-dressed atoms, *Phys. Rev. A*, **78**, 043409 (2008).

[27] J.L. Campbell and T. Papp, *At. Data Nucl. Data Tables*, **77**, 1 (2001).

[28] M. Abramowitz and I.A. Stegun, eds., *Handbook of Mathematical Functions*, Dover, New York, 1965.

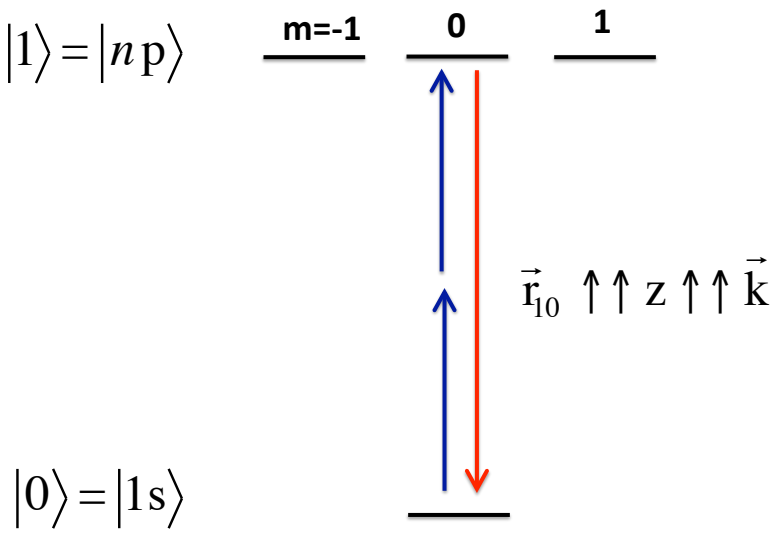

FIG. 1: The dipole moment $\mathbf{r}_{10}$ of the $1s \to np$ transition in atom is parallel to $\mathbf{k}$. The axis of quantization z is along the photon momentum $\mathbf{k}$.

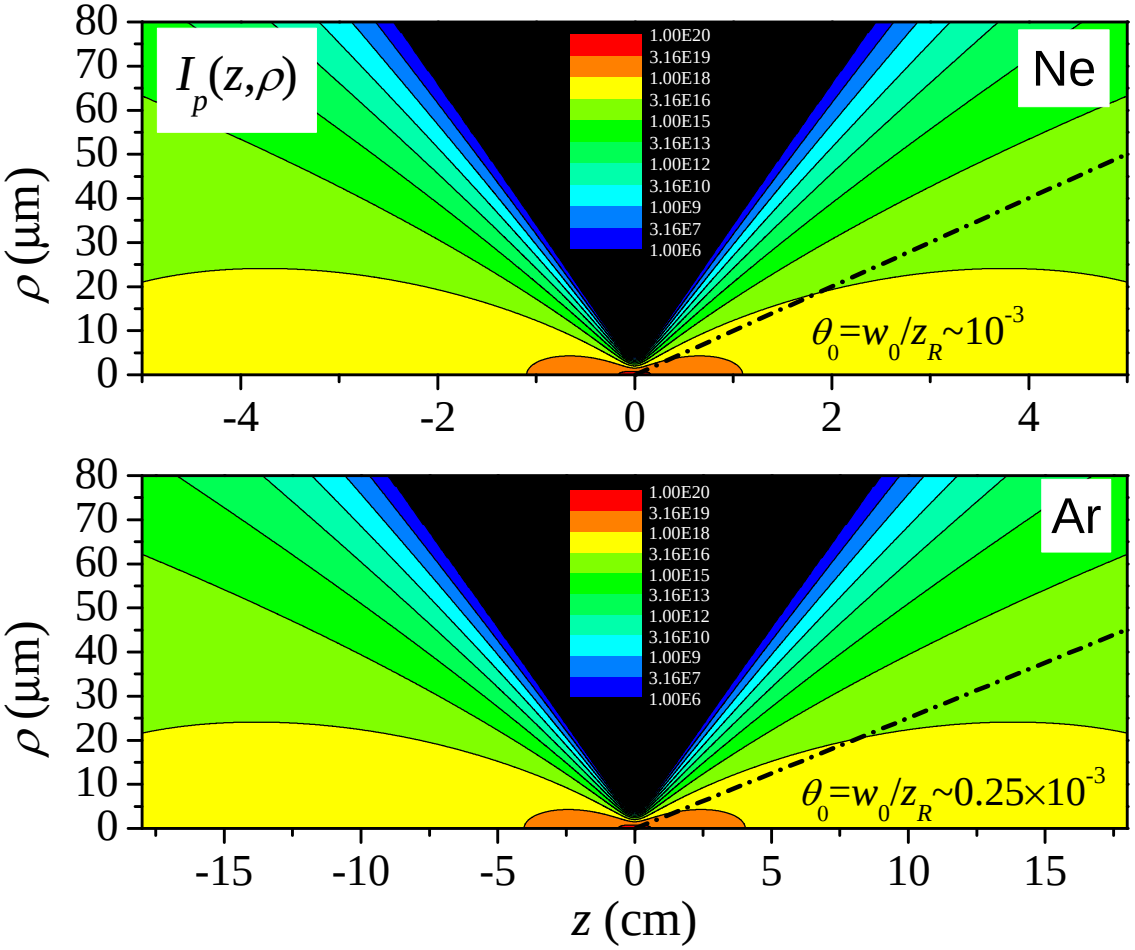

FIG. 2: 2D map of the pump intensity at $t = z/c$ for Ne and Ar. The legend shows the intensity in W/m^2.

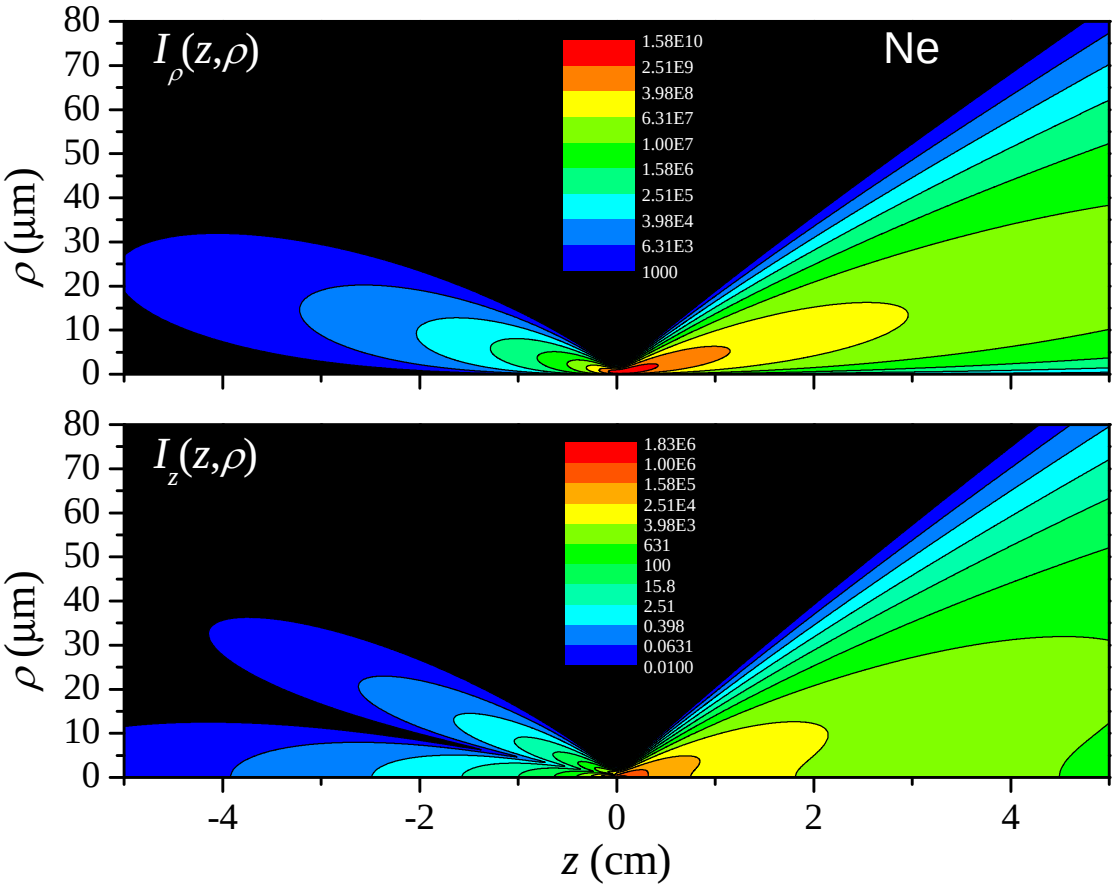

FIG. 3: 2D map of the SHG intensity at $t = z/c$ of Ne. The photoabsorption is negleted. The legend shows the intensity in W/m^2.

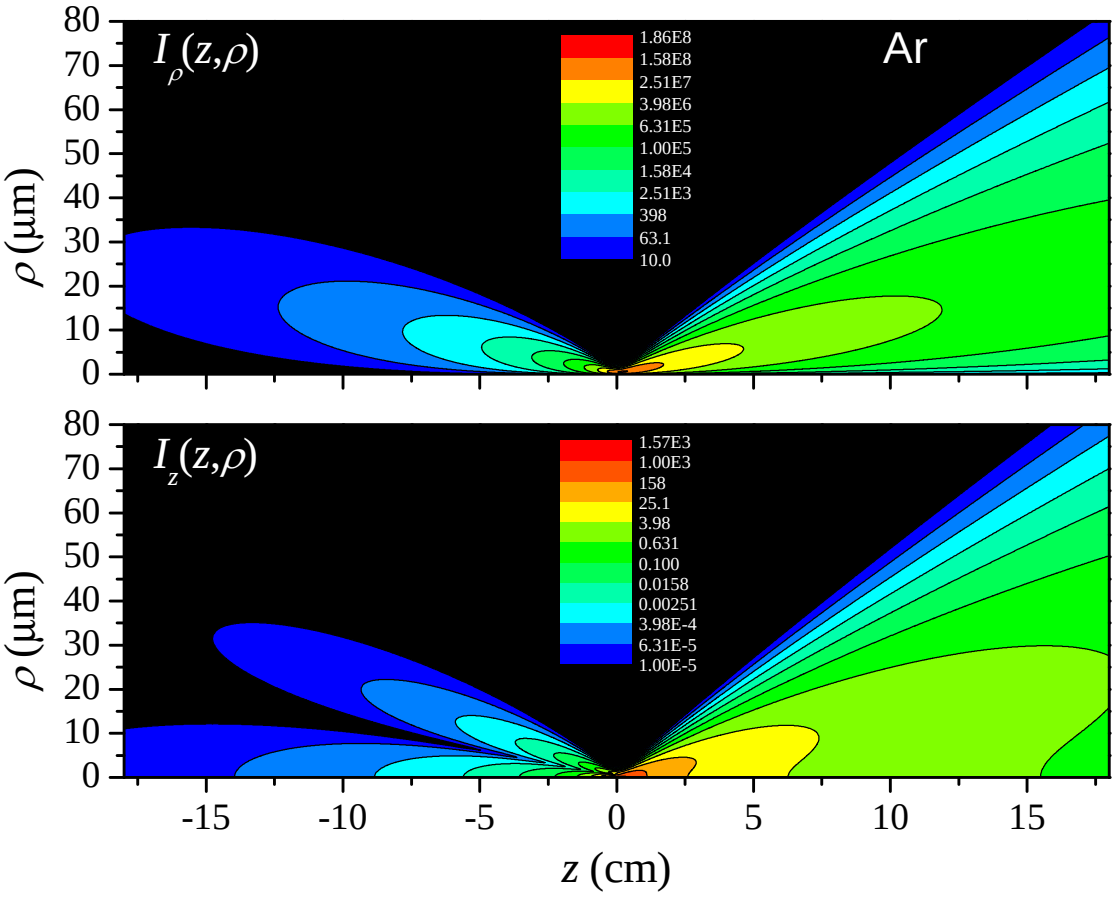

FIG. 4: 2D map of the SHG intensity at $t = z/c$ of Ar. The photoabsorption is neglected. The legend shows the intensity in W/m^2.

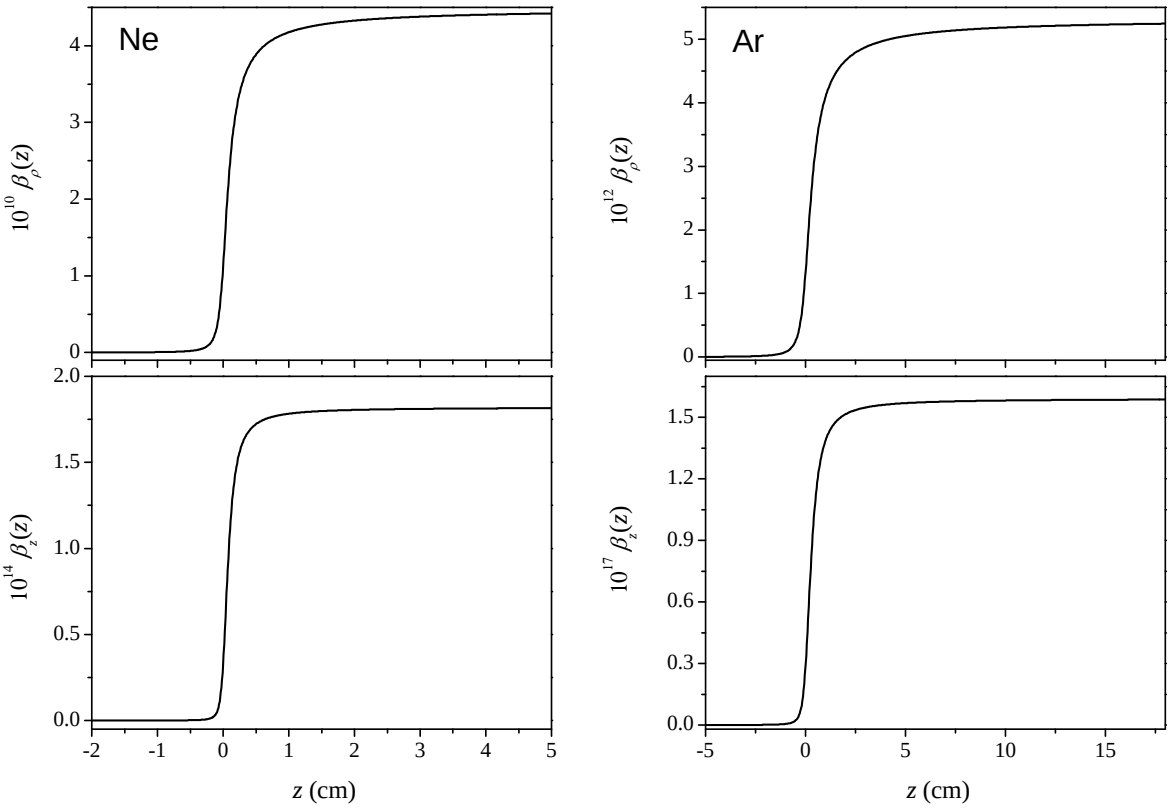

FIG. 5: Energy conversion efficiency of Ne and Ar. The photoabsorption is neglected.

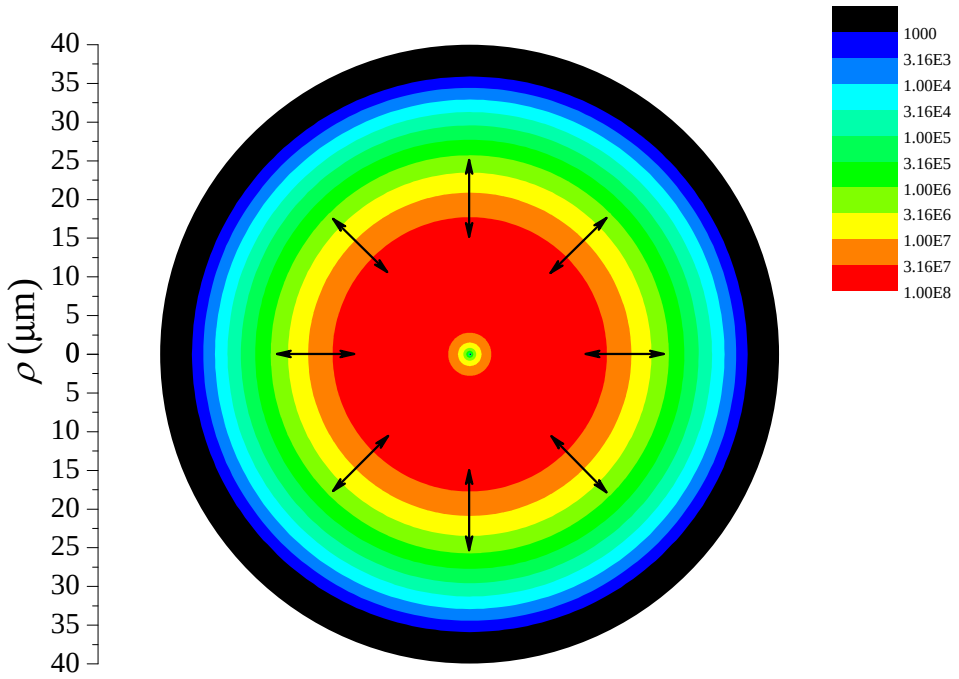

FIG. 6: Radial distribution of I_ρ for Ne at z=0.02 m. Black arrows show schematically the radially polarized SHG field.

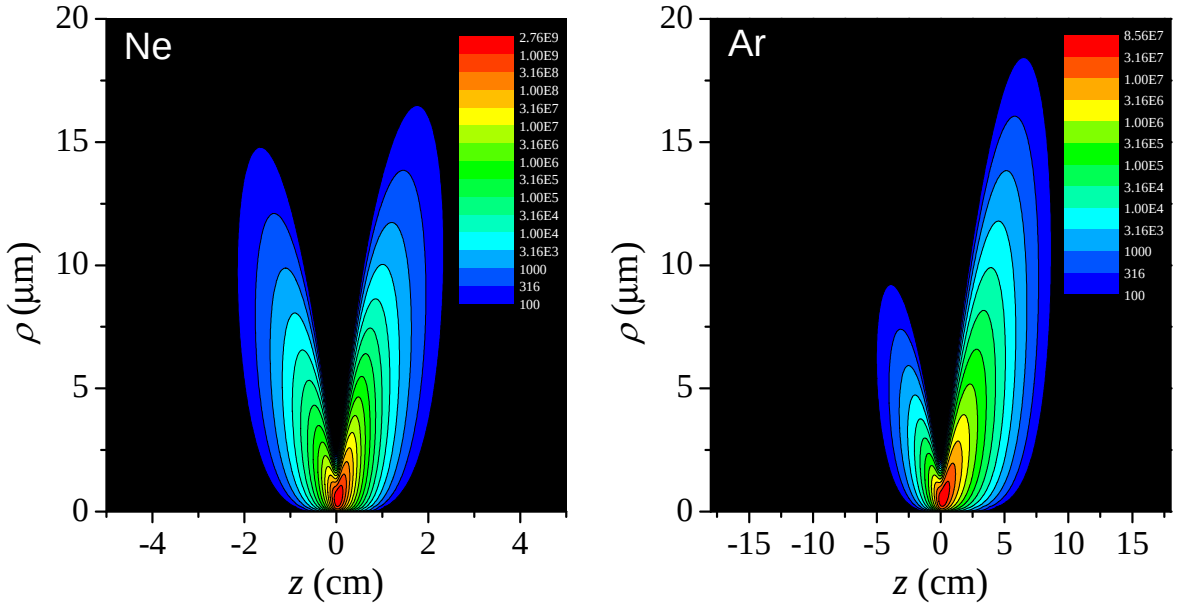

FIG. 7: Distribution of I_ρ for Ne and Ar taking into account the photoabsorption. The legend shows the intensity in W/m^2.

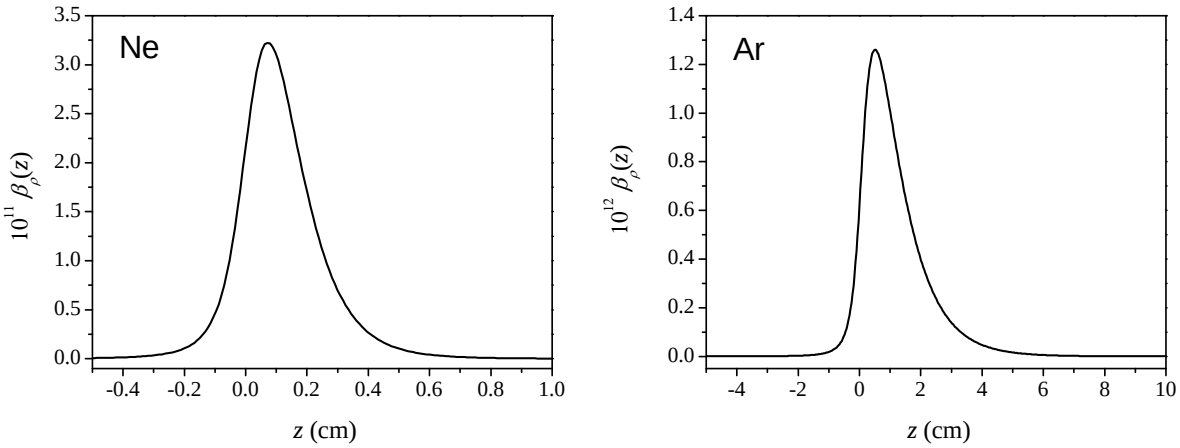

FIG. 8: Energy conversion efficiency $\beta_\rho(z)$ for Ne and Ar taking into account the photoabsorption. Ne: $\beta_\rho^{\max} = 3.2 \times 10^{-11}$ at $z_{\max} = 0.7mm$. Ar: $\beta_\rho^{\max} = 1.3 \times 10^{-12}$ at $z_{\max} = 0.5cm$.